Heading: Growing season moisture drives variation in woody productivity
Twitter: @K_A_Teixeira, @ForestGEO

1   **Title:** Growing season moisture drives inter-annual variation in woody productivity of a

2   temperate deciduous forest

3

4   **Authors**

5   Ryan Helcoski[1]

6   Alan J. Tepley[1,2,3] ORCID 0000-0002-5701-9613

7   Neil Pederson[4] ORCID 0000-0003-3830-263X

8   Jennifer C. McGarvey[1]

9   Victoria Meakem[1]

10 Valentine Herrmann[1] ORCID 0000-0002-4519-481X

11 Jonathan R. Thompson[1, 4] ORCID 0000-0003-0512-1226

12 Kristina J. Anderson-Teixeira[1, 5*] ORCID 0000-0001-8461-9713

13

14 *Corresponding author teixeirak@si.edu; 540-635-6546

15 [1]Conservation Ecology Center; Smithsonian Conservation Biology Institute; Front Royal,

16 Virginia, 22630, USA

17 [2]W. A. Franke College of Forestry & Conservation, University of Montana, Montana, 59812,

18 USA

19 [3]Division of Biological Sciences, University of Montana, Montana, 59812, USA

20 [4]Harvard Forest; Petersham, MA, 01366, USA

21 [5]Center for Tropical Forest Science-Forest Global Earth Observatory, Smithsonian Tropical

22 Research Institute, 0843-03092, Republic of Panama

23

24

Total word count (excluding summary, references and legends):	5747	No. of figures:	5 (all in colour)
Summary:	194	No. of Tables:	2
Introduction:	1054	No of Supporting Information files:	1 (Fig. S1-S14, Tables S1-S13).
Materials and Methods:	1771		.
Results:	1076		.
Discussion:	1767		
Acknowledgements:	79		

1

25

26   **Summary**

27   1. The climate sensitivity of forest ecosystem woody productivity ($ANPP_{stem}$) influences

28   carbon cycle responses to climate change. For the first time, we combine long-term

29   annual growth and forest census data of a diverse temperate broadleaf deciduous forest,

30   seeking to resolve whether $ANPP_{stem}$ is primarily moisture- or energy-limited and

31   whether climate sensitivity has changed in recent decades characterized by more mesic

32   conditions and elevated CO_2.

33   2. We analyzed tree-ring chronologies across 109 years of monthly climatic variation

34   (1901-2009) for 14 species representing 97% of $ANPP_{stem}$ in a 25.6-ha plot in northern

35   Virginia, USA.

36   3. Radial growth of most species and ecosystem-level $ANPP_{stem}$ responded positively to

37   cool, moist growing season conditions, but the same conditions in the previous May-July

38   were associated with reduced growth. In recent decades (1980-2009), responses were

39   more variable and on average, weaker.

40   4. Our results indicate that woody productivity is primarily limited by current growing

41   season moisture, as opposed to temperature or sunlight, but additional complexity in

42   climate sensitivity may reflect the use of stored carbohydrate reserves. Overall, while

43   such forests currently display limited moisture sensitivity, their woody productivity is

44   likely to decline under projected hotter and potentially drier growing season conditions.

45

46

47   **Key words:** ANPP; climate sensitivity; dendrochronology; ForestGEO; temperate deciduous

48   forest; tree rings, woody productivity, non-structural carbohydrates

49

50

Introduction

51

52   Forests globally sequester ~1/3 of anthropogenic CO_2 emissions from fossil fuel

53   combustion (Le Quéré *et al.*, 2017), thereby slowing atmospheric CO_2 accumulation and

54   consequent climate change. Yet, the persistence of this global forest carbon (C) sink is threatened

55   by climate change, including the increasing risk of severe drought (Trenberth *et al.*, 2014; Clark

56   *et al.*, 2016), and its future course remains one of the largest uncertainties in global climate

57   models (Friedlingstein *et al.*, 2006). To predict the future C balance of forests, it is necessary to

58   understand the climate sensitivity of aboveground woody net primary productivity—*i.e.,* the

59   portion of C fixed through photosynthesis that is preserved long-term in woody stems

60   ($ANPP_{stem}$). The challenge to doing so is that this requires multi-decadal records of annual

61   growth for all tree species that contribute substantively to $ANPP_{stem}$. Tree rings are invaluable for

62   disentangling the multiple interacting factors that influence growth, including climatic variation.

63   However, traditional dendrochronological methods, where only targeted canopy trees are

64   sampled, are not optimal for characterization of the climate sensitivity for entire forest stands

65   (Babst *et al.*, 2018). Moreover, and may overestimate climate sensitivity (Klesse *et al.*, 2018b).

66   There has been limited use of tree rings to estimate $ANPP_{stem}$ (Graumlich *et al.*, 1989; Davis *et*

67   *al.*, 2009; Babst *et al.*, 2014; Dye *et al.*, 2016; Klesse *et al.*, 2016; Teets *et al.*, 2018a) and its

68   climate sensitivity (Woolley *et al.*, 2015; Klesse *et al.*, 2018a; Teets *et al.*, 2018b).

69   Temperate forests are an important C sink (~0.8 Pg C yr^{-1}; Pan et al., 2011), with ~0.2 Pg

70   C sequestered annually by the broadleaf deciduous forests of eastern North America (Albani *et*

71   *al.*, 2006). Despite being among the best-studied ecosystem types on Earth (Martin *et al.*, 2012),

72   there remains large uncertainty as to the climate sensitivity of temperate broadleaf forests and

73   how they will respond to future climate change. Notably, of the >4000 collections in the

74   International Tree-Ring Databank, only 19% are of broadleaf species and of that small

75   proportion, 67% are of *Quercus* species (Zhao et al., 2019).

76   The broadleaf deciduous forests of eastern North America are generally mesic and

77   conventionally considered to be more strongly limited by energy (temperature or solar radiation)

78   than by water (Running et al., 2004). Over relatively short time scales, gross primary production

79   (GPP) and transpiration are reduced under cloudy, cool conditions (Barford, 2001; Anderson-

80   Teixeira *et al.*, 2015b). Growing season length (shaped by spring and fall temperatures) appears

81   to be a primary driver of interannual variability in net ecosystem exchange of CO_2 (NEE;

82   (Baldocchi *et al.*, 2018). Meanwhile, tree-ring based records of radial growth covering most of

83   the 20th century indicate that most of the dominant canopy species in the region respond

84   positively to water availability and negatively to high temperatures (Elliott *et al.*, 2015; Martin-

85   Benito & Pederson, 2015; Charney *et al.*, 2016; Levesque *et al.*, 2017; D'Orangeville *et al.*,

86   2018). However, it is unknown whether the whole forest ecosystem follows the trends observed

87   in tree-rings from canopy trees or whether co- and sub-dominant individuals or smaller-statured

88   species alter the response of $ANPP_{stem}$ to climatic variation (*i.e.,* a niche complementarity effect;

89   Isbell et al., 2015). Thus, it remains unclear how whole-ecosystem $ANPP_{stem}$ responds to

90   interannual variability in growing season climate.

91   Beyond the influence of current growing season conditions, $ANPP_{stem}$ is almost inevitably

92   influenced by conditions in the prior year. This is because early-season stem growth is partially

93   fueled by non-structural carbohydrate (NSC) reserves, particularly in ring porous species

94   (Trumbore *et al.*, 2002; Kagawa *et al.*, 2006; Zweifel *et al.*, 2006; Michelot *et al.*, 2012;

95   Richardson *et al.*, 2013). While NSC reserves can be decades old, the active ("fast") pool that

96   fuels new growth is typically composed of C that was fixed within the past 1-2 years (Carbone *et*

97   *al.*, 2013; Richardson *et al.*, 2013, 2015), suggesting a lagged relationship between current year

98   growth and previous years' climate conditions. These lags are common in temperate deciduous

99   species, although their direction and strength is somewhat variable (*e.g.,* Charney et al., 2016;

100   D'Orangeville et al., 2018; Hacket-Pain et al., 2018; Pederson et al., 2012). Despite the high

101   probability that $ANPP_{stem}$ is sensitive to climate conditions prior to the current growing season,

102   this sensitivity has not been characterized in most ecological studies. Characterizing the long-

103   term sensitivity of $ANPP_{stem}$ to current and previous years' climatic conditions requires scaling

104   tree-ring records from a diversity of tree sizes and species to the ecosystem level, and will be

105   critical to predicting temperate forest responses to climate change.

106   Finally, it remains unclear if and how climate sensitivity has changed in recent decades,

107   during which tree growth in US eastern deciduous forests has been altered by more mesic

108   conditions, increasing atmospheric CO_2, and declines in atmospheric pollutants (SO_x, NO_x).

109   Several studies have found that these changes drove increased tree growth within the biome, but

110   attribute the increased growth to different sets of environmental changes (McMahon *et al.*, 2010;

111   Levesque *et al.*, 2017; Mathias & Thomas, 2018). It remains unknown how such changes have

112   affected climate sensitivity in eastern US forests. In other forest biomes around the world, there

4

113   have been observations of reduced climate sensitivity in recent decades (Briffa *et al.*, 1998a,b;

114   Knapp *et al.*, 2001; Soulé & Knapp, 2006; Leal *et al.*, 2008; Wyckoff & Bowers, 2010; Maxwell

115   *et al.*, 2016), although the pattern is not universal (Biondi, 2000; Carrer & Urbinati, 2006). The

116   reductions in climate sensitivity found in some species may be attributable to increased water use

117   efficiency driven by elevated CO_2 (Briffa *et al.*, 1998a; Knapp *et al.*, 2001; Soulé & Knapp,

118   2006; Leal *et al.*, 2008; Wyckoff & Bowers, 2010), although other factors are also at play; for

119   example, in the Midwest USA, there has been a reduction in the strength of droughts in recent

120   decades (Maxwell *et al.*, 2016).

121   Here, we analyze 109 years of annual woody growth for 14 species within a temperate

122   deciduous forest in Virginia, USA to understand how multiple climate drivers influence

123   individual species growth and *ANPP*$_{stem}$. We test the hypothesis that woody growth of most

124   species and *ANPP*$_{stem}$ are primarily water-limited, as opposed to energy-limited; *i.e.,* growth

125   responds positively to growing season moisture and negatively to increased temperatures or

126   potential evapotranspiration (PET). We evaluate this hypothesis across more than a century of

127   historical climate variation (1901-2009) and for three consecutive 30-year periods therein (1920-

128   1949, 1950-1979, 1980-2009).

129

130   **Materials and Methods**

131   *Study Site*

132   Our study site was the 25.6-ha large forest dynamics plot at the Smithsonian

133   Conservation Biology Institute (SCBI) in the Blue Ridge Mountains of northern Virginia, USA

134   (Supporting Information Fig. S1; 38°53'36.6″ N, 78°08'43.4″ W; elevation 273-338 m.; Bourg,

135   McShea, Thompson, McGarvey, & Shen, 2013), which is part of the Forest Global Earth

136   Observatory (ForestGEO) network (Anderson-Teixeira *et al.*, 2015a). The climate is humid

137   temperate. From 1901 to 2009, January and July temperatures averaged 1°C and 24°C,

138   respectively, with mean annual precipitation of 998 mm distributed fairly evenly throughout the

139   year (Table 1; Supporting Information Fig. S2). Bud break typically occurs in April, and leaf

140   senescence begins in September and extends into November. Stem expansion is typically most

141   rapid between May and July. The plot is a mature secondary mixed deciduous forest that

142   developed after agricultural abandonment in the mid-19th century. Canopy trees are primarily 65

143   - 145 years old with some individuals >240 years old (Supporting Information Fig. S3a).

144

145   *Plot census and ANPP$_{stem}$ calculations*

146   The plot was censused in 2008 and 2013 using standard ForestGEO protocols, where all

147   woody stems ≥ 1 cm in diameter at breast height (DBH) were identified, mapped, tagged, and

148   measured in DBH (Condit, 1998; Bourg *et al.*, 2013). Census data, which were last updated in

149   2014, were obtained through the ForestGEO data portal (forestgeo.si.edu).

150   Census data were used to calculate mean annual *ANPP$_{stem}$* from 2008-2013. Specifically,

151   we first identified individuals that were alive in both 2008 and 2013 and estimated their

152   aboveground biomass for both years using the allometries identified in Gonzalez-Akre et al.

153   (2016) and recorded in our database of allometric equations, allodb

154   (https://github.com/forestgeo/allodb; Gonzalez-Akre, personal communication). The growth rate

155   of each individual was calculated as the difference between these values divided by the time

156   interval, using exact census dates for each tree. To identify and deal with outliers, trees were

157   grouped into DBH bins (1-5, 5-10, 10-50, >50cm) and the annual biomass increment of trees

158   deviating from the size bin mean by more than ±4 standard deviations (SD) were replaced with

159   that mean. Individual biomass growth rates were then summed across species, using minimum

160   DBH thresholds of both 1 and 10 cm.

161   Comprehensive estimation of *ANPP$_{stem}$* requires accounting for the growth of trees that

162   recruit into the census or die between censuses (Clark *et al.*, 2001). For trees that grew into the

163   ≥1 or ≥10cm DBH size class between 2008 and 2013, growth was calculated as the difference

164   between 2013 biomass and the biomass of an individual of the minimum size threshold. We

165   assumed minimal *ANPP$_{stem}$* contributions of stems that died between 2008 and 2013 because

166   trees at this site and elsewhere typically have greatly reduced growth rates for several years

167   before dying (Gonzalez-Akre *et al.*, 2016; Cailleret *et al.*, 2017). We considered the *ANPP$_{stem}$*

168   estimates including recruitment as the authoritative values for this site and used them to calculate

169   total *ANPP$_{stem}$* and contributions of each species (Table 2). However, to compare census- and

170   tree-ring- based estimates of *ANPP$_{stem}$*, we excluded recruitment, as it was not included in tree-

171   ring based estimates (Supporting Information Table S3).

172

173

174

175   *Tree core collection and chronology building*

176   We collected increment cores from a subset of trees distributed throughout the plot in

177   either 2010-11 or 2016-17 (Table 2, Supporting Information Fig. S1, Table S1). All cores were

178   taken at breast height (137 cm). In 2010-11, cores were taken from randomly selected live

179   individuals from each species with at least 30 trees ≥10 cm DBH. The majority of these were

180   subsequently measured (Bourg et al., 2013). In 2016 and 2017, we collected cores from all trees

181   found dead in our annual mortality census (Gonzalez-Akre et al., 2016). Cores were dried,

182   mounted, and sanded with a belt sander or by hand when necessary to see the cell structure

183   during periods of strong growth suppression (Speer, 2010). Rings were measured using a TA

184   Unislide Velmex (0.002 mm precision; Velmex Inc., Bloomfield, NY) for cores collected in

185   2011 and 2016. For cores collected in 2017, we used WinDENDRO (Windendro, Regent

186   Instruments Inc., Québec, Canada), having verified that these methods gave extremely similar

187   results. Ring width measurements were crossdated and verified using the program COFECHA

188   (Holmes, 1983).

189   We built crossdated chronologies for all species contributing more than 1% of $ANPP_{stem}$

190   (n=12) and two additional species, *Pinus strobus* and *Fraxinus nigra* (Table 2), which ranked

191   18th and 20th in terms of productivity contributions. Species in the top 20 contributors to

192    $ANPP_{stem}$ for which we were unable to develop accurate chronologies included *Acer rubrum,*

193   *Platanus occidentalis, Tilia americana, Nyssa sylvatica, Cercis canadensis,* and *Ulmus rubra*,

194   which each contributed <0.5% of $ANPP_{stem}$ and ranked 13th-17th and 19th in productivity,

195   respectively. Because we were interested in ecosystem-level climate sensitivity, all trees were

196   included in our final chronology; that is, we included trees whose correlations to the master

197   chronology for its species were lower than series typically used for other dendro-ecological

198   applications, such as climate reconstructions. We did not include cores from our chronologies if

199   they were degraded by decay or damaged such that deciphering ring boundaries increased

200   uncertainty in crossdating accuracy. Chronologies of trees cored live and dead were pooled

201   following analyses showing similar climate sensitivity at least up to 2009 (*i.e.*, excluding 7-8

202   years prior to death) for all four species with ≥10 cores in each category (LITU, QURU, QUVE,

203   FRAM; comparison plots available at https://github.com/SCBI-

204   ForestGEO/climate_sensitivity_cores/tree/master/results/live_vs_dead).

205   To remove or reduce nonclimatic factors related to growth (*e.g.,* geometric constraints on

206   ring width) or the influences of stand dynamics (*e.g.,* individual tree growth release and

207   suppression), all ring-width series for each species were standardized via ARSTAN using a 2/3 n

208   spline, where n is the number of years in each series (Cook, 1985; Cook & Kairiukstis, 1990).

209   We also tested a 50-year fixed width spline, which gave extremely similar results, indicating that

210   our findings are not sensitive to variable- versus fixed-width detrending. The influence of

211   outliers in all series were reduced using the adaptive power transformation, which also stabilizes

212   the variance over time (Cook & Peters, 1997). Next, each series was stabilized using either the

213   average correlation between raw ring-width series (rbar) method or a 1/3rds spline method to

214   adjust changes in variance as series replication decreased towards the earlier portion of each

215   chronology (Jones *et al.*, 1997). The 1/3rds spline method was chosen when replication in the

216   inner portion of each chronology (*ca.* the inner 30-50 years of each record depending on full

217   chronology length) dropped below three trees. Once that step was complete, a robust biweight

218   mean chronology for each species was calculated from the ring-width indices (Cook, 1985). We

219   chose to use residual chronologies because the autoregressive standardization process in creating

220   them removes much of the tree-level autocorrelation in growth and these chronologies most

221   likely contains the most conservative information on drivers of interannual growth (Cook, 1985).

222   We defined the chronology start date as the year the subsample signal strength (SSS) exceeded

223   0.75 (Table 2; Supporting Information Fig. S3b), and the end date as 2009 (thereby buffering

224   mortality events by 7-8 years). We used SSS instead of the expressed population signal (EPS)

225   because EPS can be saturated with high series replication (Buras, 2017) and we were interested

226   in climatic sensitivity, not 'quality of the tree-ring chronology' per the traditional paleoclimatic

227   approach.

228

229   *Analyses*

230   We characterized the sensitivity of growth to monthly variation in ten climate variables

231   (Table 1) from 1901 (or chronology start date, as late as 1938; Supporting Information Table S1)

232   to 2009 and over three 30-year periods covering the last 90 years of this time period (1920-49,

233   1950-79, 1980-2009). The years 1901-1919 were excluded from the analysis of shorter time

234   periods because the chronologies of several species, including the dominant *Liriodendron*

235   *tulipifera,* did not reach SSS $\geq$0.75 until 1910-20.

New Phytologist

236   Climate data were obtained from the ForestGEO Climate Data Portal

237   (https://github.com/forestgeo/Climate) in August 2018, including Climatic Research Unit

238   monthly data for eight variables from 1901 to 2016 (CRU TS v. 4.01; Harris, Jones, Osborn, &

239   Lister, 2014) and NOAA Divisional Data's Palmer Drought Severity Index (PDSI) from 1895 to

240   2017. Atmospheric CO_2 data, used as context for comparing the two time periods, was obtained

241   from a publicly available NASA data set that includes historical ice core data and NOAA ESLR

242   atmospheric data (Etheridge et al., 1996; Keeling & Whorf, 2012; National Aeronautics and

243   Space Administration, 2017; NOAA/ESRL/Global Monitoring Division, 2018). Analyses of

244   climate–growth relationships were conducted using 'dplR' (Bunn, 2008) and 'bootRes' (Zang &

245   Biondi, 2013) in R v. 3.5.1 (R Core Team, 2017), which correlation functions and bootstrapped

246   confidence intervals for the relationships between annual growth and monthly climate variables

247   following Biondi & Waikul (2004).

248   To scale from the species-level chronologies to the whole stand, we first developed

249   species-specific allometries between the average tree-ring based radial growth increment from

250   2007 to 2009 and DBH measured in the 2008 census (Supporting Information Table S2). We

251   then applied these allometries to predict radial increment for every stem ≥10 cm DBH (focal

252   species), filling in 2008-13 census growth measurements for species for which we did not have

253   chronologies (3% of $ANPP_{stem}$). Next, we combined our radial growth estimates with species-

254   specific allometries to estimate tree biomass growth and $ANPP_{stem}$. Estimates of $ANPP_{stem}$ for the

255   entire stand and for each species were compared to estimates derived from 2008-2013 census

256   data, indicating close correlation (R^2>0.99; Supporting Information Table S3). Finally, we

257   estimated the change in $ANPP_{stem}$ that would be expected under a +1 SD increase (calculated for

258   1901-2009) in the monthly values for each climate variable ($\Delta ANPP_{stem}$). Pearson correlations

259   between climate and each tree-ring chronology were converted to linear slopes as in (Charney et

260   al., 2016) and then used to predict the change in radial increment for a 1 SD increase in each

261   monthly climate variable. This coefficient was expressed relative to mean radial increment for

262   the species (Table S1) to calculate percent change under +1 SD of the climate variable. Radial

263   increment under a +1 SD increase in the climate variable was then predicted by applying this %

264   change to the radial increment predicted from allometry. For species without chronologies, we

265   assumed no climate response. Although unrealistic, this assumption is likely to have minimal

266   impact on our estimates of $ANPP_{stem}$ given the small contribution of these species to plot-level

267 $ANPP_{stem}$ (2.6%; Table 2). We computed $\Delta ANPP_{stem}$ as the difference between $ANPP_{stem}$ under

268 altered climate and that derived for baseline climate conditions, in both cases calculating

269 $ANPP_{stem}$ as described above.

270 All data, R code, and results are available through the SCBI-ForestGEO organization on

271 GitHub (https://github.com/SCBI-ForestGEO: SCBI-ForestGEO-Data and

272 climate_sensitivity_cores repositories), with static versions corresponding to data and analyses

273 presented here archived in Zenodo (DOIs: 10.5281/zenodo.2649302 and

274 10.5281/zenodo.2656633, respectively).

275

276 **Results**

277 In total, our chronologies consisted of 728 trees from 14 species and 7 genera with 16 –

278 109 cores per species (Table 2). From 2008 to 2013, these species represented 97.4% of

279 $ANPP_{stem}$ (with recruitment) for stems ≥10 cm DBH (2.83 Mg C ha^{-1} yr^{-1}; Table 2), or 96.9% of

280 $ANPP_{stem}$ for all stems ≥1cm DBH (2.87 Mg C ha^{-1} yr^{-1}).

281 The 14 species had fairly consistent inter-annual signals and differed modestly in their

282 variability (Fig. 1). Correlations between species-level residual chronologies averaged 0.41 and

283 ranged from 0.86 between *Quercus alba* and *Q. montana* to -0.032 between *Fraxinus americana*

284 and *Pinus strobus* (Supporting Information Fig. S4). Correlations between the dominant species,

285 *Liriodendron tulipifera,* and other species averaged 0.44 and ranged from 0.19 (*Fraxinus nigra*)

286 to 0.63 (*Carya covalis*). Standard deviations of the ring width index averaged 0.136 and ranged

287 from 0.10 (*Quercus rubra, Fraxinus americana*) to 0.18 (*Juglans nigra, Carya tomentosa*; Table

288 S1).

289 Over the centennial time scale, species' climate responses were broadly indicative of

290 water-, as opposed to energy-, limitation (Figs. 1-2, Supporting Information Figs. S5-S14, Tables

291 S4-13). Species generally responded positively to current peak growing season (May-August)

292 moisture (rain day frequency, precipitation, PDSI) and cloudiness, while responding negatively

293 to temperature (max, mean, min), daily temperature range, PET, and PET-PRE. This held true

294 for 92.7% of all climate variable-month combinations, with 36% of the relationships significant

295 at p<0.05. Species also responded positively to April temperatures (max, mean, min) and PET

296 (82.1% of species-variable combinations, 11% significant). Responses to previous May-July

297 conditions tended to be opposite those of the current growing season (75.7% of species-variable-

10

298   month combinations, 19% significant), tending to be most pronounced in *Quercus* spp. (Figs. 2,

299   S5-S14). However, responses to conditions in August and September of the previous growing

300   season were more similar to those of the current growing season; growth was generally higher

301   under cloudy, wet conditions with favorable water balance (CLD, PRE, WET, PDSI; 74.1% of

302   species-variable-month combinations), but responses of energy variables (temperature, DTR,

303   PET, PET-PRE) were not consistent (56.5% of species-variable-month combinations). The

304   species deviating most commonly from the above-described patterns were the two contributing

305   <1% of $ANPP_{stem}$: *Fraxinus nigra*, most individuals of which grow along streams or in other

306   persistently wet microsites, and *Pinus strobus*, a conifer and also the species with the shortest

307   chronology (Fig. 1).

308   The climate sensitivity of each species' growth and $ANPP_{stem}$—*i.e.*, % change in

309   individual growth or $ANPP_{stem}$ for +1SD change in climate—mirrored the observed Pearson

310   correlations while also scaling with the SD of chronologies (Fig. 2). In other words, for the same

311   strength of correlation with a climate variable under current climate, the growth and $ANPP_{stem}$ of

312   species with higher growth variability (*e.g., Juglans nigra, Carya tomatosa*) was more sensitive

313   to increases in the climate variable than those with low growth variability (*e.g., Quercus rubra,*

314   *Fraxinus americana*). Growth sensitivities ranged up to ~ ±5% for each species- climate

315   variable- month combination, but on average were much less, including for the dominant species,

316   *Liriodendron tulipifera* (Fig. 2). While <5% is a modest response, we note that it applies to only

317   a +1 SD change in one climate variable for one month, whereas a notably hot or dry growing

318   season may involve changes >2 SDs over several months, resulting in a larger growth response.

319   Scaled to the ecosystem level, $ANPP_{stem}$ reflected the dominant climate responses

320   described above (Fig. 2-3)—particularly those of *Liriodendron tulipifera*, which contributed by

321   far the most to stand-level $ANPP_{stem}$ (Fig. 2i). $ANPP_{stem}$ was generally most sensitive to

322   conditions in the current peak growing season and to moisture of the previous May. The most

323   influential variables (by month) included current May PET-PRE, PET, and wet day frequency,

324   ±1 SD variation in which affected $ANPP_{stem}$ by >0.05 Mg ha^{-1} yr^{-1} (>1.8% of total; Fig. 3).

325   Responses were somewhat buffered relative to those of *Liriodendron tulipifera,* for which the

326   strongest responses were slightly greater than ±2.5%.

327   The three 30-year time periods selected for comparison differed somewhat in climatic

328   and atmospheric conditions. Climatically, 1950-1979 was most similar to the average conditions

329 over 1901-2009, with more drought in the early 20th century (1920-49) and more mesic

330 conditions in recent decades (Fig. 1; Supporting Information Fig. S2). Specifically, 1980-2009

331 was characterized by slightly higher than average cloud cover and PDSI and a narrower range of

332 daily temperatures, whereas the reverse was true of 1920-49 (Supporting Information Fig. S2).

333 Of the ten years with the largest difference between PET and precipitation during May-July, two

334 occurred in 1980-2009 (ranked 8th and 10th in magnitude), with 3 each in the other time periods

335 (ranked 1st – 6th in magnitude with the two largest in 1920-49; Fig. 1). Atmospherically, recent

336 decades were characterized by higher atmospheric CO_2 (average of 361 ppm) compared to

337 previous periods (308 ppm for 1920-49, 322 ppm for 1950-79) and the full time period (325

338 ppm).

339 Over recent decades (1980-2009), species' climate responses were more variable and less

340 pronounced compared to both the full time period (1901-2009) and the two earlier 30-year time

341 periods (1920-49, 1950-79; Fig. 4; Supporting Information Figs. S5-S14, Tables S4-13). Most

342 notably, from 1980-2009 there were fewer positive species' responses to moisture (CLD, WET,

343 PRE, PDSI) and fewer negative responses to temperatures, DTR, PET, and PET-PRE (70% of

344 species-variable-month combinations, 5% significant; compared with 83-93% in the other 3 time

345 periods; Fig. 4a). The average strength of these correlations was also notably reduced in recent

346 decades relative to earlier decades and the full 110-year time frame (Fig. 4; Supporting

347 Information Figs. S5-S14, Tables S4-13). Consistency of responses to April temperatures and

348 PET and previous May-July conditions were likewise reduced (59% and 41% with same sign of

349 correlation coefficients as the trends described above, respectively; Fig. 4a). Also, over the last

350 three decades, responses to conditions in August and September of the previous growing season

351 switched from moisture-dominated to temperature-dominated (Fig. 4a); growth was not

352 consistently higher under cloudy, wet conditions (54% of species-variable-month combinations),

353 whereas temperature and PET responses were predominantly negative (72% of species-variable-

354 month combinations).

355 Similarly, *ANPP*$_{stem}$ was generally less responsive to climate over recent decades (1980-

356 2009) than during 1920-49, 1950-79, or the entire 109 analysis time frame (Figs. 3,5). This

357 largely reflected the responses of *Liriodendron tulipifera* (LITU; 48% of *ANPP*$_{stem}$; Fig. 2i),

358 which tended to have relatively weak responses to growing season climate from 1980-2009

359 compared to some other species (Supporting Information Figs. S5-S14), but was also consistent

360 with the overall weakening of climate sensitivity across species (Fig. 4).

361

362

363 **Discussion**

364 In the first study to scale from species-level to the climate sensitivity of $ANPP_{stem}$

365 (ecosystem-level) in a diverse broadleaf-dominated temperate deciduous forest, we show that

366 radial growth of 14 tree species and ecosystem-level $ANPP_{stem}$ respond positively to cool, moist

367 growing season conditions for >92% of month-variable combinations over 109 years of variable

368 climatic conditions (Figs. 1-3). These responses generally remained the same in structure across

369 three 30-year periods, but were more variable and less pronounced during recent decades (1980–

370 2009) at both individual and ecosystem scales ($ANPP_{stem}$; Figs. 4-5). There was also a tendency,

371 again less consistent over recent decades, for the lagged relationship between the current year's

372 growth and climate during the previous May-July to be opposite that of the current growing

373 season (Figs. 2-3, 5). That is, growth was reduced by cool, moist conditions during the previous

374 May-July. This, together with commonly negative responses to high temperatures from late

375 summer of the preceding year through current early spring (Figs. 2-3, 5; Supporting Information

376 Figs. S5-S7), could indicate a key role of NSC reserves. Thus, building off of species-level

377 research, we show that $ANPP_{stem}$ of a humid temperate forest is also primarily limited by

378 moisture, as opposed to temperature or sunlight, but that carbohydrate reserves from the previous

379 year contribute to a more complex climate sensitivity.

380 Responses to the ten climate variables analyzed were largely consistent across species

381 (Figs. 1-2), and therefore the climate sensitivity of $ANPP_{stem}$ (Fig. 3) reflected that of most

382 individual species. There was a modest niche complementarity effect (Figs. 2-3), implying that,

383 in this forest, species diversity slightly increases the stability of $ANPP_{stem}$ under fluctuating

384 climate conditions, as has been observed in other plant communities worldwide (Isbell *et al.*,

385 2015; Anderegg *et al.*, 2018). However, the similar responses across species imply that

386 biophysical constraints have bound species' climate sensitivities within a relatively narrow range

387 and limited the potential for biodiversity to buffer substantially against climate extremes. An

388 additional implication is that in forests such as this with relatively low topographic complexity

389 and the majority of $ANPP_{stem}$ concentrated within several dominant species (here, 5 species

390   account for 80% of $ANPP_{stem}$; Table 1), the climate sensitivity of $ANPP_{stem}$ can be satisfactorily

391   characterized based on tree-ring chronologies of those dominant species.

392   Forest woody productivity ($ANPP_{stem}$) was strongly influenced by current growing season

393   conditions, being highest under relatively cool, low-PET, cloudy conditions with frequent

394   precipitation (Figs. 2-3). This agrees with other tree-ring studies across eastern US deciduous

395   forests showing positive moisture responses of tree growth (Belmecheri *et al.*, 2014; Elliott *et al.*,

396   2015; Martin-Benito & Pederson, 2015; Charney *et al.*, 2016; Levesque *et al.*, 2017).

397   Physiologically, the observed positive response of radial growth to wet conditions is consistent

398   with the fact that the proximate driver of stem growth is hydraulically-driven cell expansion

399   (Zweifel et al., 2006), with most rapid stem diameter increases on rainy days (Herrmann et al.,

400   2016). Subsequent C sequestration associated with cell wall thickening can lag by more than a

401   month (Cuny et al., 2015), implying that the climate sensitivities of stem growth and

402   photosynthesis are at least partially decoupled in time within the current growing season. Thus,

403   observations of negative responses of temperate moist deciduous forest GPP (Barford *et al.*,

404   2001) and sap flow (Anderson-Teixeira *et al.*, 2015b) to cool, wet conditions over time scales of

405   days to months are not inconsistent with the observed positive response of annual stem growth to

406   inter-annual variation in moisture.

407   In contrast to the negative impact of temperature during the growing season, tree growth

408   and $ANPP_{stem}$ responded positively to high April temperatures, indicative of thermal limitations

409   to the start of the growing season and consistent with other tree-ring observations in the central

410   Appalachians (Mathias & Thomas, 2018) and with findings that GPP and NEE (White *et al.*,

411   1999; Baldocchi *et al.*, 2018) are sensitive to growing season length. However, the influence of

412   April temperatures on $ANPP_{stem}$ was quite modest relative to conditions in May-August and even

413   the previous early growing season (Fig. 3).

414   The relationship between current year's growth and climate prior to the current growing

415   season is likely due to spring and early summer stem growth being partially fueled, at least in

416   part, by NSC reserves—particularly in ring-porous species (~48% of $ANPP_{stem}$ in our plot; Table

417   2; Zweifel *et al.*, 2006; Michelot *et al.*, 2012). We suggest three possible mechanisms behind the

418   observed inverse responses to past May-July conditions (Figs. 2-3, Supporting Information Figs.

419   S5-S14). First, at this site, tree transpiration, and by extension photosynthesis, are reduced on

420   humid, cloudy days (Anderson-Teixeira *et al.*, 2015b), whereas stem expansion is essentially

421   twice as rapid on rainy days than rainless days (Herrmann et al., 2016). Thus, on the time scale

422   of one to a few days, GPP and $ANPP_{stem}$ respond differentially to climatic conditions, but it

423   remains unknown how these climate sensitivities scale to monthly or annual time scales. Second,

424   wet conditions early in the growing season may drive greater stem expansion and, subsequently,

425   higher C demand for cell wall thickening, potentially resulting in less surplus C for NSC storage

426   and lower growth the following year. Finally, NSCs may be preferentially allocated to other

427   functions (*e.g.,* reproduction)—and away from stem growth—based on previous year growing

428   conditions (Hacket-Pain et al., 2018). Research will be needed to test the hypotheses that NSC

429   reserves at the beginning of the growing season may influence $ANPP_{stem}$ and its climate

430   sensitivity. Regardless, the dependency of stem growth on prior climate implies that, while tree-

431   ring analysis is invaluable for inferring the climate sensitivity of $ANPP_{stem}$, these relationships

432   must be combined with physiological data and models to characterize climatic drivers of total

433   forest C sequestration.

434   In recent decades, we observed two notable shifts in the climate sensitivities of woody

435   growth and $ANPP_{stem}$. First, the consistency of the relationship between tree growth and moisture

436   became muted compared to that found over the full 109-year record (Figs. 4-5). This weakening

437   of the climate–growth relationship was at least partially driven by slightly more mesic conditions

438   with fewer strong droughts (Fig. 1, Supplementary Information Fig. S2), with a similar trend

439   noted across several sites in the Midwest US (Maxwell *et al.*, 2016) and evidence that more

440   mesic conditions have been associated with increased growth in the Northeast US (Levesque *et*

441   *al.*, 2017). It is also possible that elevated CO_2 has an interactive effect on climate sensitivity,

442   buffering growth responses in drought years by increasing water use efficiency (Levesque *et al.*,

443   2017; Mathias & Thomas, 2018), while having less or no impact on growth during wet years

444   (Knapp *et al.*, 2001; Soulé & Knapp, 2006; Wyckoff & Bowers, 2010; Levesque *et al.*, 2017).

445   Further research will be required to fully understand the mechanisms driving the observed

446   declines in the strength of climate–growth relationships. However, whatever the mechanism, this

447   observation is significant for our understanding of the ecophysiology of North American

448   temperate deciduous forests in that they appear to be less moisture-limited at present than they

449   have been in the past or are likely to be in the future (Clark *et al.*, 2016). Current

450   ecophysiological research on these forests (*e.g.,* eddy-covariance studies, extensive forest

451   monitoring, model parameterization and evaluation) is therefore capturing a period of low

452   drought stress and likely under-estimating the importance of moisture for forest ecosystem

453   productivity.

454   Second, at least on the ecosystem level ($ANPP_{stem}$), the relative importance of climatic

455   conditions prior to the start of the growing season appears to have increased, in part because of

456   decreasing influence of current growing season conditions (Fig. 4-5). This also points to

457   increasing decoupling between the climate sensitivities of $ANPP_{stem}$ and GPP, implying that

458   responses of woody growth to current growing season climatic conditions are not currently a

459   reliable indicator of the climate sensitivity of ecosystem C sequestration.

460   Our results suggest that the woody productivity of forests such as ours is likely to decline

461   under expected future climate conditions. Future projections for the region include increased

462   temperatures (~1-5 °C by 2100, depending on emissions; IPCC, 2014), with associated increases

463   in PET and evaporative demand likely to more than offset predicted slight (≤10%) increases in

464   precipitation (IPCC, 2013, 2014; U.S. Global Change Research Program, 2014; Cook *et al.*,

465   2015). The negative effects of high temperatures and PET on growth (Fig. 2; Supporting

466   Information Figs. S5-S9) and $ANPP_{stem}$ (Fig. 3) indicate that increasing temperatures will likely

467   reduce forest productivity by increasing evaporative demand and water limitation, aligning with

468   the conclusions of other temperate deciduous forest tree-ring studies (*e.g.,* Charney *et al.*, 2016;

469   Klesse *et al.*, 2018). Moreover, our finding that wet day frequency had an overall greater

470   importance than total precipitation implies that any shift in precipitation distribution into fewer,

471   larger storms is also likely to have a negative impact on tree growth (Elliott *et al.*, 2015). These

472   effects could be somewhat buffered by increased water use efficiency under elevated CO_2, and

473   understanding the extent to which this may be occurring remains an important open question.

474   While the CO_2 effect on growth overall may be weak in eastern US deciduous forests (Levesque

475   et al., 2017) and globally (Peñuelas *et al.*, 2011), this does not rule out a meaningful impact

476   during drier years—as has been observed in other regions (Knapp *et al.*, 2001; Soulé & Knapp,

477   2006; Wyckoff & Bowers, 2010). However, even if the weakening of climate–growth

478   relationships in recent decades observed here (Figs. 4-5) is attributable to increased water use

479   efficiency under elevated CO_2, the effect is unlikely to be sufficient to prevent productivity

480   declines under projected future climate conditions (Charney *et al.*, 2016).

481   Our pairing of tree-ring analyses with plot data yields a long-term perspective on climate

482   sensitivity of $ANPP_{stem}$. Without such long-term data, it is impossible to disentangle the

16

483   sometimes-subtle influence of climate on tree growth. As we show, the longer time frame can

484   reveal sensitivities that are not being detected by contemporary high-resolution forest

485   measurements (*e.g.,* eddy flux, dendrometer bands) that serve as the basis for most forest

486   ecosystem-climate models. Importantly, the processes that appear to be governing growth in this

487   study are not well represented in current models, most of which forecast an overall enhancement

488   of forest productivity with projected climate change (Albani *et al.*, 2006; Ollinger *et al.*, 2008;

489   Duveneck & Thompson, 2017). We have yet to characterize interactive effects among climate

490   variables (Foster *et al.*, 2016) or variables known to influence climate sensitivity, including tree

491   size (Bennett *et al.*, 2015), canopy position (Teets *et al.*, 2018b), topographic position (Elliott *et*

492   *al.*, 2015), and competition (D'Amato *et al.*, 2013). Incorporating these factors in future analyses

493   will further strengthen predictions of $ANPP_{stem}$ and its responses to climate variability and

494   change.

495

496   **Acknowledgements**

503

504   **Author Contributions**

505   KAT, RH, AT, and NP designed the research. Cores were collected and measured by JM (2010-

506   11), VM (2016), and RH (2017) under guidance of JRT (2010-11), KAT and AT (2016-17).

507   Chronologies were developed by RH under guidance of AT and NP. Data analyses were

508   performed by performed by VH under guidance of KAT, AT, and NP. KAT, RH, AT, and NP

509   interpreted the results. RH and KAT wrote the first draft of manuscript, and all authors (RH,

510   KAT, AT, NP, JM, VM, JRT & VH) contributed to revisions.

511

512   **References**

513   **Albani M, Medvigy D, Hurtt GC, Moorcroft PR**. **2006**. The contributions of land-use change,
514   CO2 fertilization, and climate variability to the Eastern US carbon sink. *Global Change Biology*
515   **12**: 2370–2390.

516   **Anderegg WRL, Konings AG, Trugman AT, Yu K, Bowling DR, Gabbitas R, Karp DS, Pacala S,**
517   **Sperry JS, Sulman BN,** *et al.* **2018**. Hydraulic diversity of forests regulates ecosystem resilience
518   during drought. *Nature* **561**: 538.

519   **Anderson-Teixeira KJ, Davies SJ, Bennett AC, Gonzalez-Akre EB, Muller-Landau HC, Joseph**
520   **Wright S, Abu Salim K, Almeyda Zambrano AM, Alonso A, Baltzer JL,** *et al.* **2015a**. CTFS-
521   ForestGEO: a worldwide network monitoring forests in an era of global change. *Global Change*
522   *Biology* **21**: 528–549.

523   **Anderson-Teixeira KJ, Mcgarvey JC, Muller-Landau HC, Park JY, Gonzalez-Akre EB, Herrmann**
524   **V, Bennett AC, So C V., Bourg NA, Thompson JR,** *et al.* **2015b**. Size-related scaling of tree form
525   and function in a mixed-age forest. *Functional Ecology* **29**: 1587–1602.

526   **Babst F, Bodesheim P, Charney N, Friend AD, Girardin MP, Klesse S, Moore DJP, Seftigen K,**
527   **Björklund J, Bouriaud O,** *et al.* **2018**. When tree rings go global: Challenges and opportunities
528   for retro- and prospective insight. *Quaternary Science Reviews* **197**: 1–20.

529   **Babst F, Bouriaud O, Alexander R, Trouet V, Frank D**. **2014**. Toward consistent measurements
530   of carbon accumulation: A multi-site assessment of biomass and basal area increment across
531   Europe. *Dendrochronologia* **32**: 153–161.

532   **Baldocchi D, Chu H, Reichstein M**. **2018**. Inter-annual variability of net and gross ecosystem
533   carbon fluxes: A review. *Agricultural and Forest Meteorology* **249**: 520–533.

534   **Barford CC**. **2001**. Factors Controlling Long- and Short-Term Sequestration of Atmospheric CO2
535   in a Mid-latitude Forest. *Science* **294**: 1688–1691.

536   **Barford CC, Wofsy SC, Goulden ML, Munger JW, Pyle EH, Urbanski SP, Hutyra L, Saleska SR,**
537   **Fitzjarrald D, Moore K**. **2001**. Factors Controlling Long- and Short-Term Sequestration of
538   Atmospheric CO2 in a Mid-latitude Forest. *Science* **294**: 1688–1691.

539   **Belmecheri S, Maxwell RS, Taylor AH, Davis KJ, Freeman KH, Munger WJ**. **2014**. Tree-ring
540    $\updelta$ 13C tracks flux tower ecosystem productivity estimates in a NE temperate forest.
541   *Environmental Research Letters* **9**: 074011.

542   **Bennett AC, McDowell NG, Allen CD, Anderson-Teixeira KJ**. **2015**. Larger trees suffer most
543   during drought in forests worldwide. *Nature Plants* **1**: 15139.

544   **Biondi F**. **2000**. Are Climate-Tree Growth Relationships Changing in North-Central Idaho, U.S.A.?
545   *Arctic, Antarctic, and Alpine Research* **32**: 111–116.

546   **Biondi F, Waikul K**. **2004**. DENDROCLIM2002: A C++ program for statistical calibration of
547   climate signals in tree-ring chronologies. *Computers & Geosciences* **30**: 303–311.

548   **Bourg NA, McShea WJ, Thompson JR, McGarvey JC, Shen X**. **2013**. Initial census, woody
549   seedling, seed rain, and stand structure data for the SCBI SIGEO Large Forest Dynamics Plot.
550   *Ecology* **94**: 2111–2112.

551   **Briffa KR, Schweingruber FH, Jones PD, Osborn TJ, Harris IC, Shiyatov SG, Vaganov EA, Grudd**
552   **H**. **1998a**. Trees tell of past climates: but are they speaking less clearly today? (DJ Beerling, WG
553   Chaloner, and FI Woodward, Eds.). *Philosophical Transactions of the Royal Society of London.*
554   *Series B: Biological Sciences* **353**: 65–73.

555   **Briffa KR, Schweingruber FH, Jones PD, Osborn TJ, Shiyatov SG, Vaganov EA**. **1998b**. Reduced
556   sensitivity of recent tree-growth to temperature at high northern latitudes. *Nature* **391**: 678.

557   **Bunn AG**. **2008**. A dendrochronology program library in R (dplR). *Dendrochronologia* **26**: 115–
558   124.

559   **Buras A**. **2017**. A comment on the expressed population signal. *Dendrochronologia* **44**: 130–
560   132.

561   **Cailleret M, Jansen S, Robert EMR, Desoto L, Aakala T, Antos JA, Beikircher B, Bigler C,**
562   **Bugmann H, Caccianiga M, *et al.* 2017**. A synthesis of radial growth patterns preceding tree
563   mortality. *Global Change Biology* **23**: 1675–1690.

564   **Carbone MS, Czimczik CI, Keenan TF, Murakami PF, Pederson N, Schaberg PG, Xu X,**
565   **Richardson AD**. **2013**. Age, allocation and availability of nonstructural carbon in mature red
566   maple trees. *New Phytologist* **200**: 1145–1155.

567   **Carrer M, Urbinati C**. **2006**. Long-term change in the sensitivity of tree-ring growth to climate
568   forcing in Larix decidua. *New Phytologist* **170**: 861–872.

569   **Charney ND, Babst F, Poulter B, Record S, Trouet VM, Frank D, Enquist BJ, Evans MEK**. **2016**.
570   Observed forest sensitivity to climate implies large changes in 21st century North American
571   forest growth. *Ecology letters* **19**: 1119–1128.

572   **Clark DA, Brown S, Kicklighter DW, Chambers J, Thomlinson JR, Ni J**. **2001**. Measuring net
573   primary production in forests: concepts and field methods. *Ecological Applications* **11**: 356–370.

574   **Clark JS, Iverson L, Woodall CW, Allen CD, Bell DM, Bragg DC, D'Amato AW, Davis FW, Hersh**
575   **MH, Ibanez I, *et al.* 2016**. The impacts of increasing drought on forest dynamics, structure, and
576   biodiversity in the United States. *Global change biology* **22**: 2329–2352.

577   **Condit RS**. **1998**. *Tropical Forest Census Plots - Methods and Results from Barro Colorado Island,*
578   *Panama and a Comparison with Other Plots*. Springer-Verlag, Berlin, and R. G. Landes Company,
579   Georgetown, TX, USA.

580   **Cook ER**. **1985**. A Time Series Analysis Approach to Tree Ring Standardization, PhD diss.,
581   University of Arizona: 37-73.

582   **Cook BI, Ault TR, Smerdon JE**. **2015**. Unprecedented 21st century drought risk in the American
583   Southwest and Central Plains. *Science Advances* **1**: e1400082.

584   **Cook ER, Kairiukstis LA**. **1990**. *Methods of Dendrochronology: Applications in the Environmental*
585   *Sciences*. Dordrecht: Kluwer Academic Publishers.

586   **Cook ER, Peters K**. **1997**. Calculating unbiased tree-ring indices for the study of climatic and
587   environmental change. *The Holocene* **7**: 361–370.

588   **Cuny HE, Rathgeber CBK, Frank D, Fonti P, Mäkinen H, Prislan P, Rossi S, del Castillo EM,**
589   **Campelo F, Vavrčík H,** *et al.* **2015**. Woody biomass production lags stem-girth increase by over
590   one month in coniferous forests. *Nature Plants* **1**: 15160.

591   **D'Amato AW, Bradford JB, Fraver S, Palik BJ**. **2013**. Effects of thinning on drought vulnerability
592   and climate response in north temperate forest ecosystems. *Ecological Applications* **23**: 1735–
593   1742.

594   **Davis SC, Hessl AE, Scott CJ, Adams MB, Thomas RB**. **2009**. Forest carbon sequestration
595   changes in response to timber harvest. *Forest Ecology and Management* **258**: 2101–2109.

596   **D'Orangeville L, Maxwell J, Kneeshaw D, Pederson N, Duchesne L, Logan T, Houle D,**
597   **Arseneault D, Beier CM, Bishop DA,** *et al.* **2018**. Drought timing and local climate determine
598   the sensitivity of eastern temperate forests to drought. *Global Change Biology* **24**: 2339–2351.

599   **Duveneck MJ, Thompson JR**. **2017**. Climate change imposes phenological trade-offs on forest
600   net primary productivity. *Journal of Geophysical Research: Biogeosciences* **122**: 2298–2313.

601   **Dye A, Plotkin AB, Bishop D, Pederson N, Poulter B, Hessl A**. **2016**. Comparing tree-ring and
602   Permanent plot estimates of aboveground net primary production in three eastern U.S. forests.
603   *Ecosphere* **7**: 1–13.

604   **Elliott KJ, Miniat CF, Pederson N, Laseter SH**. **2015**. Forest tree growth response to
605   hydroclimate variability in the southern Appalachians. *Global Change Biology* **21**: 4627–4641.

606   **Etheridge D, Steele L, Langenfelds R, Francy R, Barnola J, Morgan V**. **1996**. Natural and
607   anthropogenic changes in atmospheric CO2 over the last 1000 years from air in Antarctic ice
608   and firn. *JGR Atmospheres* **101**: 4115–4128.

609   **Foster JR, Finley AO, D'Amato AW, Bradford JB, Banerjee S**. **2016**. Predicting tree biomass
610   growth in the temperate–boreal ecotone: Is tree size, age, competition, or climate response
611   most important? *Global Change Biology* **22**: 2138–2151.

20

612   **Friedlingstein P, Cox P, Betts R, Bopp L, von Bloh W, Brovkin V, Cadule P, Doney S, Eby M,**
613   **Fung I, et al. 2006**. Climate–Carbon Cycle Feedback Analysis: Results from the C4MIP Model
614   Intercomparison. *Journal of Climate* **19**: 3337–3353.

615   **Gonzalez-Akre E, Meakem V, Eng CY, Tepley AJ, Bourg NA, McShea W, Davies SJ, Anderson-**
616   **Teixeira K. 2016**. Patterns of tree mortality in a temperate deciduous forest derived from a
617   large forest dynamics plot. *Ecosphere* **7**: 1-12

618   **Graumlich LJ, Brubaker LB, Grier CC. 1989**. Long-term trends in forest net primary productivity:
619   Cascade Mountains, Washington. *Ecology* **70**: 405–410.

620   **Hacket-Pain AJ, Ascoli D, Vacchiano G, Biondi F, Cavin L, Conedera M, Drobyshev I, Liñán ID,**
621   **Friend AD, Grabner M, et al. 2018**. Climatically controlled reproduction drives interannual
622   growth variability in a temperate tree species. *Ecology Letters* **21**: 1833–1844.

623   **Harris I, Jones PD, Osborn TJ, Lister DH. 2014**. Updated high-resolution grids of monthly
624   climatic observations - the CRU TS3.10 Dataset: UPDATED HIGH-RESOLUTION GRIDS OF
625   MONTHLY CLIMATIC OBSERVATIONS. *International Journal of Climatology* **34**: 623–642.

626   **Herrmann V, McMahon SM, Detto M, Lutz JA, Davies SJ, Chang-Yang C-H, Anderson-Teixeira**
627   **KJ. 2016**. Tree Circumference Dynamics in Four Forests Characterized Using Automated
628   Dendrometer Bands. *PloS one* **11**: e0169020.

629   **Holmes RL. 1983**. Computer-assisted quality control in tree-ring dating and measurement. *Tree-*
630   *Ring Bulletin* **43**: 69–78.

631   **IPCC. 2013**. *Climate Change 2013: The Physical Science Basis. Contribution of Working Group I*
632   *to the Fifth Assessment Report of the Intergovernmental Panel on Climate Change* (TF Stocker, D
633   Quin, G-K Plattner, M Tignor, SK Allen, J Boschung, A Nauels, Y Xia, V Bex, and PM Midgley,
634   Eds.). Cambridge, UK and New York, NY, USA: Cambridge University Press.

635   **IPCC. 2014**. *Climate change 2014: impacts, adaptation, and vulnerability: Working Group II*
636   *contribution to the fifth assessment report of the Intergovernmental Panel on Climate Change*
637   (VR Barros and CB Field, Eds.). New York, NY: Cambridge University Press.

638   **Isbell F, Craven D, Connolly J, Loreau M, Schmid B, Beierkuhnlein C, Bezemer TM, Bonin C,**
639   **Bruelheide H, Luca E de, et al. 2015**. Biodiversity increases the resistance of ecosystem
640   productivity to climate extremes. *Nature* **526**: 574–577.

641   **Jones PD, Osborn TJ, Briffa KR. 1997**. Estimating Sampling Errors in Large-Scale Temperature
642   Averages. *Journal of Climate* **10**: 2548–2568.

643   **Kagawa A, Sugimoto A, Maximov TC. 2006**. 13CO2 pulse-labelling of photoassimilates reveals
644   carbon allocation within and between tree rings. *Plant, Cell & Environment* **29**: 1571–1584.

645 **Keeling CD, Whorf TP**. **2012**. Atmospheric CO2 Records from Sites in the SIO Air Sampling
646 Network. https://cdiac.ess-dive.lbl.gov/trends/co2/sio-keel.html

647 **Klesse S, Babst F, Lienert S, Spahni R, Joos F, Bouriaud O, Carrer M, Filippo AD, Poulter B,**
648 **Trotsiuk V,** *et al.* **2018a**. A combined tree-ring and vegetation model assessment of European
649 forest growth sensitivity to inter-annual climate variability. *Global Biogeochemical Cycles* **32**:
650 1226-1240.

651 **Klesse S, DeRose RJ, Guiterman CH, Lynch AM, O'Connor CD, Shaw JD, Evans MEK**. **2018b**.
652 Sampling bias overestimates climate change impacts on forest growth in the southwestern
653 United States. *Nature Communications* **9**: 5336.

654 **Klesse S, Etzold S, Frank D**. **2016**. Integrating tree-ring and inventory-based measurements of
655 aboveground biomass growth: research opportunities and carbon cycle consequences from a
656 large snow breakage event in the Swiss Alps. *European Journal of Forest Research* **135**: 297–
657 311.

658 **Knapp PA, Soulé PT, Grissino-Mayer HD**. **2001**. Detecting potential regional effects of increased
659 atmospheric CO2 on growth rates of western juniper. *Global Change Biology* **7**: 903–917.

660 **Leal S, Eamus D, Grabner M, Wimmer R, Cherubini P**. **2008**. Tree rings of Pinus nigra from the
661 Vienna basin region (Austria) show evidence of change in climatic sensitivity in the late 20th
662 century. *Canadian Journal of Forest Research* **38**: 744–759.

663 **Levesque M, Andreu-Hayles L, Pederson N**. **2017**. Water availability drives gas exchange and
664 growth of trees in northeastern US, not elevated CO_2 and reduced acid deposition. *Scientific*
665 *Reports* **7**: 46158.

666 **Martin LJ, Blossey B, Ellis E**. **2012**. Mapping where ecologists work: biases in the global
667 distribution of terrestrial ecological observations. *Frontiers in Ecology and the Environment* **10**:
668 195–201.

669 **Martin-Benito D, Pederson N**. **2015**. Convergence in drought stress, but a divergence of
670 climatic drivers across a latitudinal gradient in a temperate broadleaf forest. *Journal of*
671 *Biogeography* **42**: 925–937.

672 **Mathias JM, Thomas RB**. **2018**. Disentangling the effects of acidic air pollution, atmospheric
673 CO2, and climate change on recent growth of red spruce trees in the Central Appalachian
674 Mountains. *Global Change Biology* **24**: 3938–3953.

675 **Maxwell JT, Harley GL, Robeson SM**. **2016**. On the declining relationship between tree growth
676 and climate in the Midwest United States: the fading drought signal. *Climatic Change* **138**: 127–
677 142.

678 **McMahon SM, Parker GG, Miller DR**. **2010**. Evidence for a recent increase in forest growth.
679 *Proceedings of the National Academy of Sciences* **107**: 3611–3615.

680   **Michelot A, Simard S, Rathgeber C, Dufrêne E, Damesin C**. **2012**. Comparing the intra-annual
681   wood formation of three European species (Fagus sylvatica, Quercus petraea and Pinus
682   sylvestris) as related to leaf phenology and non-structural carbohydrate dynamics. *Tree*
683   *Physiology* **32**: 1033–1045.

684   **National Aeronautics and Space Administration**. **2017**. Global Mean CO2 Mixing Ratios (ppm):
685   Observations. https://data.giss.nasa.gov/modelforce/ghgases/Fig1A.ext.txt. 1 March 2019.

686   **NOAA/ESRL/Global Monitoring Division**. **2018**. NOAA ESRL DATA.
687   https://www.esrl.noaa.gov/gmd/. 1 March 2019.

688   **Ollinger SV, Goodale CL, Hayhoe K, Jenkins JP**. **2008**. Potential effects of climate change and
689   rising CO2 on ecosystem processes in northeastern U.S. forests. *Mitigation and Adaptation*
690   *Strategies for Global Change* **13**: 467–485.

691   **Pan Y, Birdsey RA, Fang J, Houghton R, Kauppi PE, Kurz WA, Phillips OL, Shvidenko A, Lewis SL,**
692   **Canadell JG, *et al.* 2011**. A Large and Persistent Carbon Sink in the World's Forests. *Science* **333**:
693   988–993.

694   **Pederson N, Bell AR, Cook ER, Lall U, Devineni N, Seager R, Eggleston K, Vranes KP**. **2012**. Is an
695   Epic Pluvial Masking the Water Insecurity of the Greater New York City Region?,. *Journal of*
696   *Climate* **26**: 1339–1354.

697   **Peñuelas J, Canadell JG, Ogaya R**. **2011**. Increased water-use efficiency during the 20th century
698   did not translate into enhanced tree growth. *Global Ecology and Biogeography* **20**: 597–608.

699   **Le Quéré C, Andrew RM, Friedlingstein P, Sitch S, Pongratz J, Manning AC, Korsbakken JI,**
700   **Peters GP, Canadell JG, Jackson RB, *et al.* 2017**. Global Carbon Budget 2017. *Earth System*
701   *Science Data Discussions* **10**: 1–79.

702   **R Core Team**. **2017**. R: A language and environment for statistical computing. R Foundation for
703   Statistical Computing, Vienna, Austria. URL http://www.R-project.org/.

704   **Richardson AD, Carbone MS, Huggett BA, Furze ME, Czimczik CI, Walker JC, Xu X, Schaberg**
705   **PG, Murakami P**. **2015**. Distribution and mixing of old and new nonstructural carbon in two
706   temperate trees. *New Phytologist* **206**: 590–597.

707   **Richardson AD, Carbone MS, Keenan TF, Czimczik CI, Hollinger DY, Murakami P, Schaberg PG,**
708   **Xu X**. **2013**. Seasonal dynamics and age of stemwood nonstructural carbohydrates in temperate
709   forest trees. *New Phytologist* **197**: 850–861.

710   **Running S, Nemani R, Heinsch F, Zhao M, Reeves M, Hashimoto H**. **2004**. A Continuous
711   Satellite-Derived Measure of Global Terrestrial Primary Production. *BioScience* **54**: 547–560.

712   **Soulé PT, Knapp PA**. **2006**. Radial growth rate increases in naturally occurring ponderosa pine
713   trees: a late-20th century CO2 fertilization effect? *New Phytologist* **171**: 379–390.

714   **Speer JH**. **2010**. *Fundamentals of Tree-Ring Research*. Tucson, Arizona: The University of Arizona
715   Press.

716   **Teets A, Fraver S, Hollinger DY, Weiskittel AR, Seymour RS, Richardson AD**. **2018a**. Linking
717   annual tree growth with eddy-flux measures of net ecosystem productivity across twenty years
718   of observation in a mixed conifer forest. *Agricultural and Forest Meteorology* **249**: 479–487.

719   **Teets A, Fraver S, Weiskittel AR, Hollinger DY**. **2018b**. Quantifying climate–growth
720   relationships at the stand level in a mature mixed-species conifer forest. *Global Change Biology*
721   **24**: 3587–3602.

722   **Trenberth KE, Dai A, van der Schrier G, Jones PD, Barichivich J, Briffa KR, Sheffield J**. **2014**.
723   Global warming and changes in drought. *Nature Climate Change* **4**: 17–22.

724   **Trumbore S, Gaudinski JB, Hanson PJ, Southon JR**. **2002**. Quantifying ecosystem-atmosphere
725   carbon exchange with a 14C label. *Eos, Transactions American Geophysical Union* **83**: 265–268.

726   **U.S. Global Change Research Program**. **2014**. *Climate change impacts in the United States : U.S.*
727   *national climate assessment*. https://www.globalchange.gov/browse/reports/climate-change-
728   impacts-united-states-third-national-climate-assessment-0. 27 July 2019.

729   **White MA, Running SW, Thornton PE**. **1999**. The impact of growing-season length variability on
730   carbon assimilation and evapotranspiration over 88 years in the eastern US deciduous forest.
731   *International Journal of Biometeorology* **42**: 139–145.

732   **Woolley TJ, Harmon ME, O'Connell KB**. **2015**. Inter-annual variability and spatial coherence of
733   net primary productivity across a western Oregon Cascades landscape. *Forest Ecology and*
734   *Management* **335**: 60–70.

735   **Wyckoff PH, Bowers R**. **2010**. Response of the prairie–forest border to climate change: impacts
736   of increasing drought may be mitigated by increasing CO2. *Journal of Ecology* **98**: 197–208.

737   **Zang C, Biondi F**. **2013**. Dendroclimatic calibration in R: The bootRes package for response and
738   correlation function analysis. *Dendrochronologia* **31**: 68–74.

739   **Zhao S, Pederson N, D'Orangeville L, HilleRisLambers J, Boose E, Penone C, Bauer B, Jiang Y,**
740   **Manzanedo RD**. **2019**. The International Tree-Ring Data Bank (ITRDB) revisited: Data availability
741   and global ecological representativity. *Journal of Biogeography* **46**: 355-368

742   **Zweifel R, Zimmermann L, Zeugin F, Newbery DM**. **2006**. Intra-annual radial growth and water
743   relations of trees: implications towards a growth mechanism. *Journal of Experimental Botany*
744   **57**: 1445–1459.

745

746 **Supporting Information**

747 Additional supporting information may be found in the online version of this article.

748 **Figure S1** Map of trees cored in the 26-ha SCBI ForestGEO plot and analyzed in this study.

749 **Figure S2** Monthly means ± SD of climate variables over the four time frames analyzed here

750 **Figure S3** Numbers of cores and SSS through time for chronologies analyzed here.

751 **Figure S4** Matrix of correlation between species chronologies.

752 **Figure S5** Species responses to TMX.

753 **Figure S6** Species responses to TMP.

754 **Figure S7** Species responses to TMN.

755 **Figure S8** Species responses to DTR.

756 **Figure S9** Species responses to PET.

757 **Figure S10** Species responses to PET-PRE.

758 **Figure S11** Species responses to PDSI.

759 **Figure S12** Species responses to PRE.

760 **Figure S13** Species responses to WET.

761   **Figure S14** Species responses to CLD.

762 **Table S1** Chronology details, including n cores and chronology statistics.

763 **Table S2** Species-specific allometries between radial increment and DBH

764 **Table S3** Comparison of ANPP_stem estimates from census data and cores.

765 **Table S4** Summary of Pearson correlations with TMX for all species.

766 **Table S5** Summary of Pearson correlations with TMP for all species.

767 **Table S6** Summary of Pearson correlations with TMN for all species.

768 **Table S7** Summary of Pearson correlations with DTR for all species.

769   **Table S8** Summary of Pearson correlations with PET for all species.

770   **Table S9** Summary of Pearson correlations with PET-PRE for all species.

771   **Table S10** Summary of Pearson correlations with PDSI for all species.

772   **Table S11** Summary of Pearson correlations with PRE for all species.

773   **Table S12** Summary of Pearson correlations with WET for all species.

774   **Table S13** Summary of Pearson correlations with CLD for all species.

775   Table 1. Climate variables analyzed here, along with their January and July means.

			1901 - 2009 mean ± SD	
Variable	Code	Units	January	July
average daily maximum temperature	TMX	°C	7.0 ± 2.7	31.2 ± 1.2
average daily mean temperature	TMP	°C	1.1 ± 2.6	24.2 ± 1.0
average daily minimum temperature	TMN	°C	-4.8 ± 2.5	17.3 ± 0.9
diurnal temperature range	DTR	°C	11.7 ± 0.9	13.9 ± 1.1
potential evapotranspiration	PET	mm day^{-1}	1.3 ± 0.2	4.4 ± 0.4
potential evapotranspiration - precipitation	PET-PRE	mm mo^{-1}	-31.2 ± 35.3	31.4 ± 44.5
Palmer Drought Severity Index*	PDSI	-	-0.19 ± 2.01	0.08 ± 1.94
precipitation	PRE	mm mo^{-1}	71 ± 33	104 ± 37
wet day frequency	WET	mo^{-1}	12.8 ± 2.7	11.2 ± 1.9
cloud cover	CLD	%	69 ± 3	62 ± 6

776   *Higher values indicate wetter conditions. Values were pre-whitened for analysis.

777

778   Table 2. Species analyzed here, their contributions to aboveground woody net primary

779   productivity (*ANPP*$_{stem}$) within the Smithsonian Conservation Biology Institute (SCBI)

780   ForestGEO plot (stems ≥10cm; 2008-2013), and key features of their chronologies.

Species	Species code	Ring porosity	*ANPP*$_{stem}$ Mg C * ha^{-1} yr^{-1}	%	n cores	Chronology $\overline{DBH}_{2008}$ ** (min, max)	SD of RWI[†]
Liriodendron tulipifera	LITU	diffuse	1.349	47.61	109	32.7 (10.0, 97.6)	0.14
Quercus alba	QUAL	ring	0.305	10.77	66	42.9 (11.3, 76.7)	0.12
Quercus rubra	QURU	ring	0.288	10.17	71	49.4 (10.1, 137)	0.10
Quercus velutina	QUVE	ring	0.217	7.66	83	50.6 (16.0, 109)	0.13
Quercus montana	QUPR	ring	0.136	4.80	67	38.1 (10.2, 84.6)	0.14
Fraxinus americana	FRAM	ring	0.107	3.77	69	33.3 (5.8. 93.0)	0.10
Carya glabra	CAGL	ring	0.103	3.62	39	26.6 (10.2, 52.3)	0.10
Juglans nigra	JUNI	semi-ring	0.060	2.12	31	43.4 (20.4, 76.2)	0.18
Carya tomentosa	CATO	ring	0.055	1.95	17	24.0 (12.0, 44.4)	0.18
Carya cordiformis	CACO	ring	0.055	1.93	18	23.9 (10.4, 60.5)	0.13
Fagus grandifolia	FAGR	diffuse	0.040	1.43	81	19.9 (10.1, 103)	0.15
Carya ovalis	CAOVL	ring	0.031	1.10	24	32.9 (15.1, 60.3)	0.11
Pinus strobus	PIST	-	0.007	0.25	36	28.8 (15.0, 51.0)	0.16
Fraxinus nigra	FRNI	ring	0.005	0.18	16	19.4 (6.9, 38.4)	0.15
all other species	-	-	0.075	2.64	-	-	-

781   * Mg C ha^{-1} yr^{-1} refers to Megagrammes (or tonnes) of Carbon per Hectare per Year

782   ** $\overline{DBH}_{2008}$ refers to the mean Diameter at Breast Height of tree species in 2008

783   † SD of RWI refers to the Standard Deviation of Ring-Width Index

784

785

786   **Figure Legends**

787

788   Figure 1. Residual chronologies of 14 tree species, including the 12 largest contributors to

789   Aboveground woody Net Primary Productivity ($ANPP_{stem}$) in the Smithsonian Conservation

790   Biology Institute (SCBI) ForestGEO plot, from 1901-2009. Also shown is mean May-July

791   potential evapotranspiration (PET; mm mo^{-1}) and precipitation (PRE; mm mo^{-1}), with dashed

792   vertical lines indicating the ten years in which the difference between the two was greatest

793   (1911: 83mm, 1914: 82mm, 1930: 112mm, 1936: 85mm, 1944: 89mm; 1964: 84mm, 1966:

794   83mm, 1977: 87mm, 1999: 80mm, 2007: 82mm). Species are shown in descending order of their

795   contributions to $ANPP_{stem}$. Chronologies are shown starting when Subsample Signal Strength

796   (SSS) ≥0.75 (Table S1). Refer to Table 2 for species specific code information.

797

798   Figure 2. Species' responses to four of the most influential climate variables analyzed here—

799   potential evapotranspiration (a,b) wet day frequency (c,d), the difference between potential

800   evapotranspiration and precipitation (e,f), and maximum temperature (g,h). Shown are Pearson

801   correlations between ring width index and monthly climate variables (left panel) and percent

802   response of growth and Aboveground woody Net Primary Productivity ($ANPP_{stem}$) to +1

803   Standard Deviation (SD) in the climate variable (right panel). Also shown is $ANPP_{stem}$ of each

804   species (i). Refer to Table 2 for species specific code information.

805

806   Figure 3. Sensitivity of Aboveground woody Net Primary Productivity ($ANPP_{stem}$) to 10 climate

807   variables from 1901-2009. Shown is change in $ANPP_{stem}$ (Mg C ha^{-1} yr^{-1} and % of total) with +1

808   Standard Deviation (SD) in climate variable, as predicted based on the responses of individual

809   species and the 2008 census of the Smithsonian Conservation Biology Institute (SCBI)

810   ForestGEO plot.

811

812   Figure 4. Comparison of the (a) consistency and (b) average strength of climate correlations

813   across the time periods analyzed here. Panel (a) shows the percent of species-climate variable-

814   month combinations for which Pearson correlations are positive for moisture variables (PRE,

815   WET, PDSI, CLD) and negative for energy variables (TMAX, TMP, TMIN, DTR, PET, PET-

816   PRE) in each of 3 time periods: previous year's early growing season (mjj), previous year's late

817   growing season (as), and current peak growing season (MJJA). Panel (b) shows the mean

818   absolute correlation of growth to several climate variables of all species over MJJA. Refer to

819   Table 1 for explanations of moisture and energy variables.

820

821   Figure 5. Predicted response of Aboveground woody Net Primary Productivity ($ANPP_{stem}$) to +1

822   Standard Deviation (SD) change in 10 climate variables, as predicted based on the responses of

823   individual species over three 30-year time periods and the 2008 census of the Smithsonian

824   Conservation Biology Institute (SCBI) ForestGEO plot.

826   Figure 1.
827

828
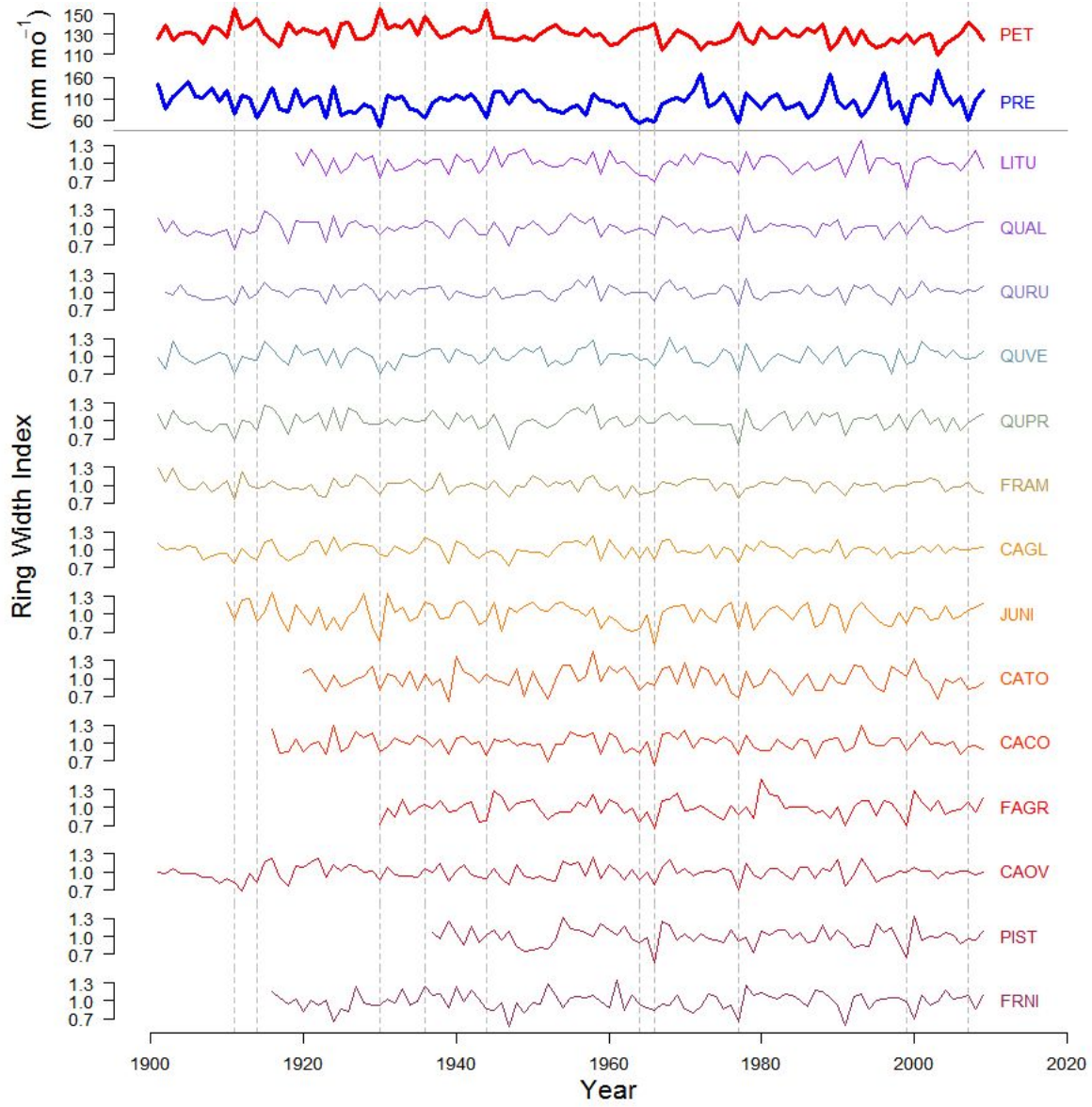
829   Figure 2.
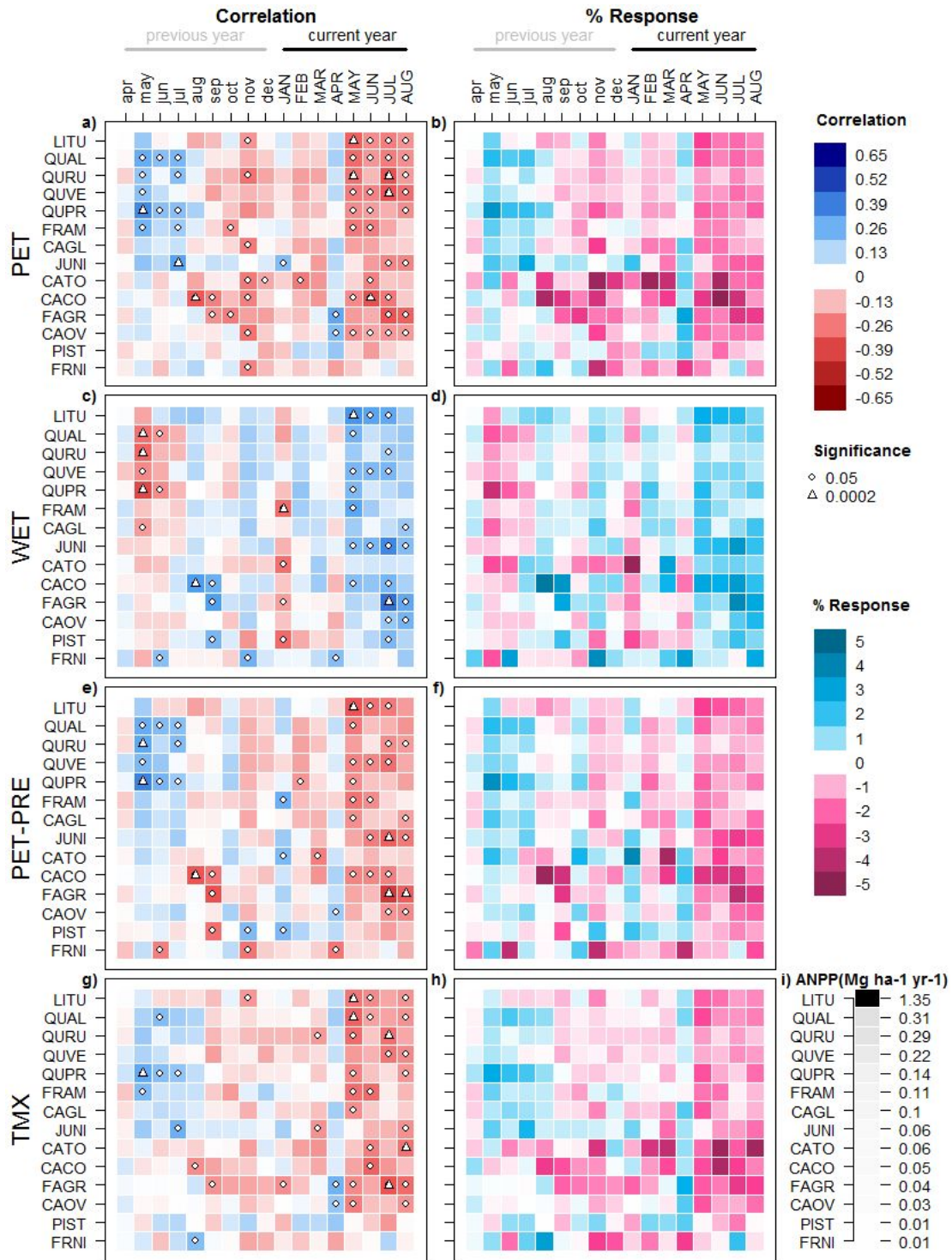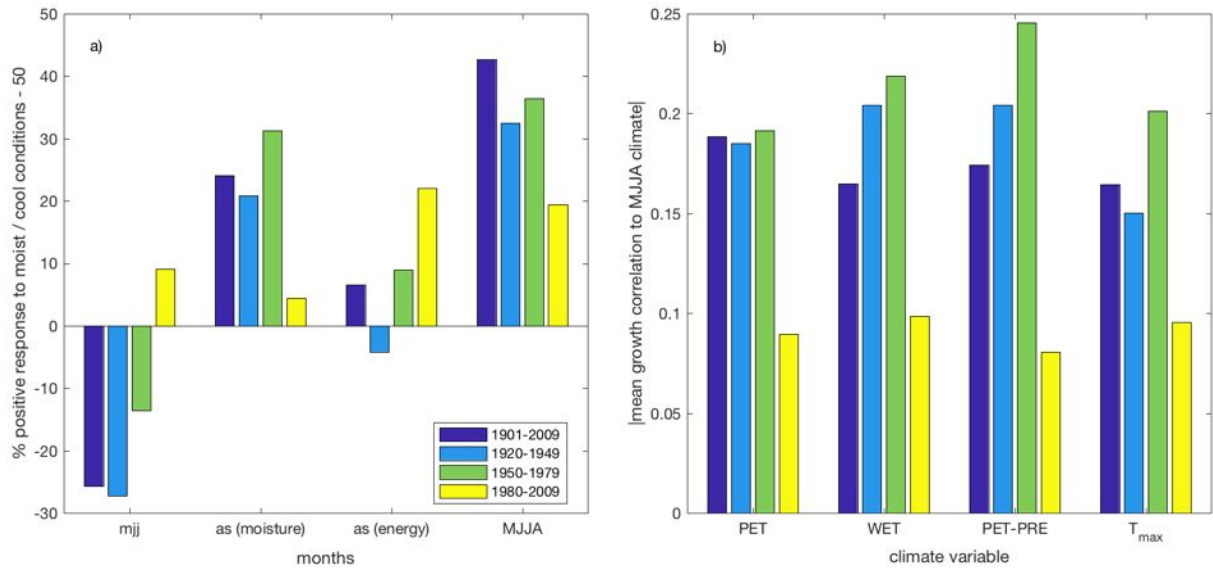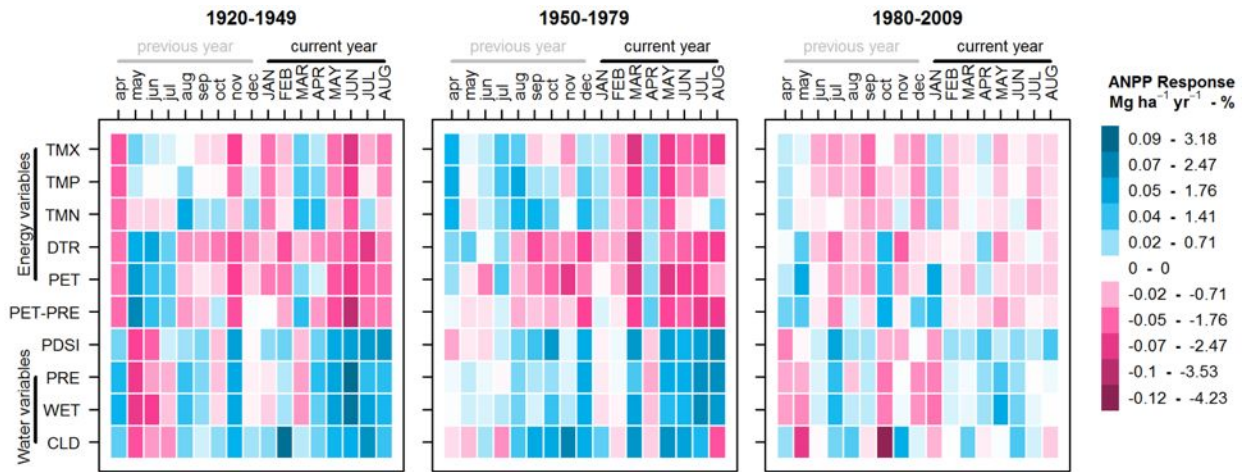
831   Figure 3.

832
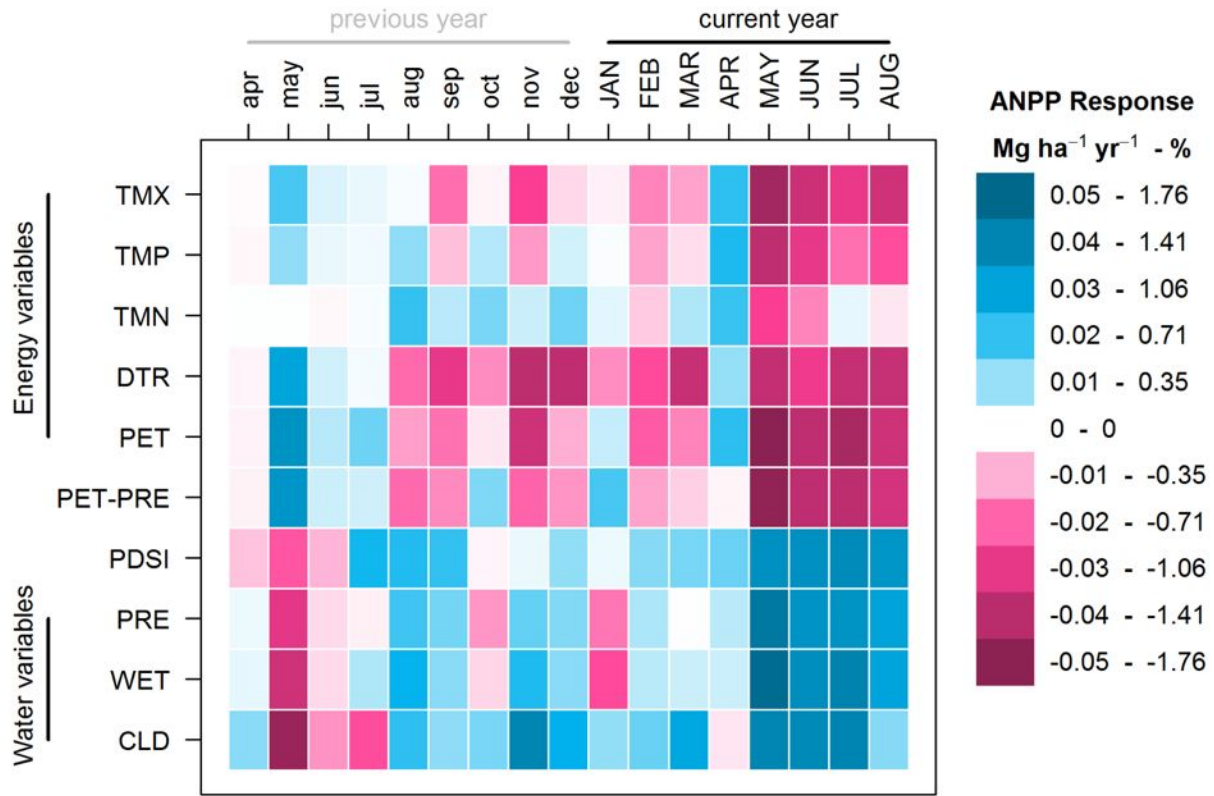
833

834

835   Figure 4.
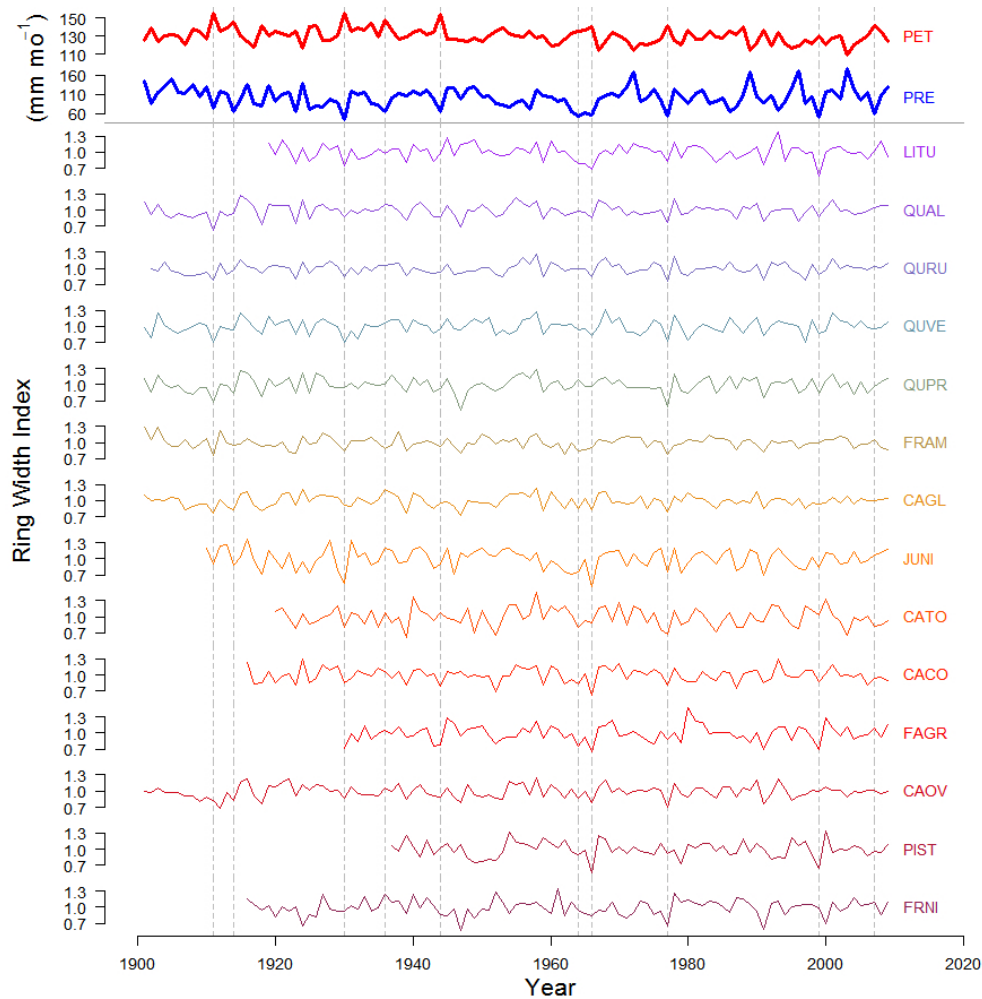

836

837

838   Figure 5.

839

Figure 1. Residual chronologies of 14 tree species, including the 12 largest contributors to Aboveground woody Net Primary Productivity (ANPPstem) in the Smithsonian Conservation Biology Institute (SCBI) ForestGEO plot, from 1901-2009. Also shown is mean May-July potential evapotranspiration (PET; mm mo-1) and precipitation (PRE; mm mo-1), with dashed vertical lines indicating the ten years in which the difference between the two was greatest (1911: 83mm, 1914: 82mm, 1930: 112mm, 1936: 85mm, 1944: 89mm; 1964: 84mm, 1966: 83mm, 1977: 87mm, 1999: 80mm, 2007: 82mm). Species are shown in descending order of their contributions to ANPPstem. Chronologies are shown starting when Subsample Signal Strength (SSS) ≥0.75 (Table S1). Refer to Table 2 for species specific code information.
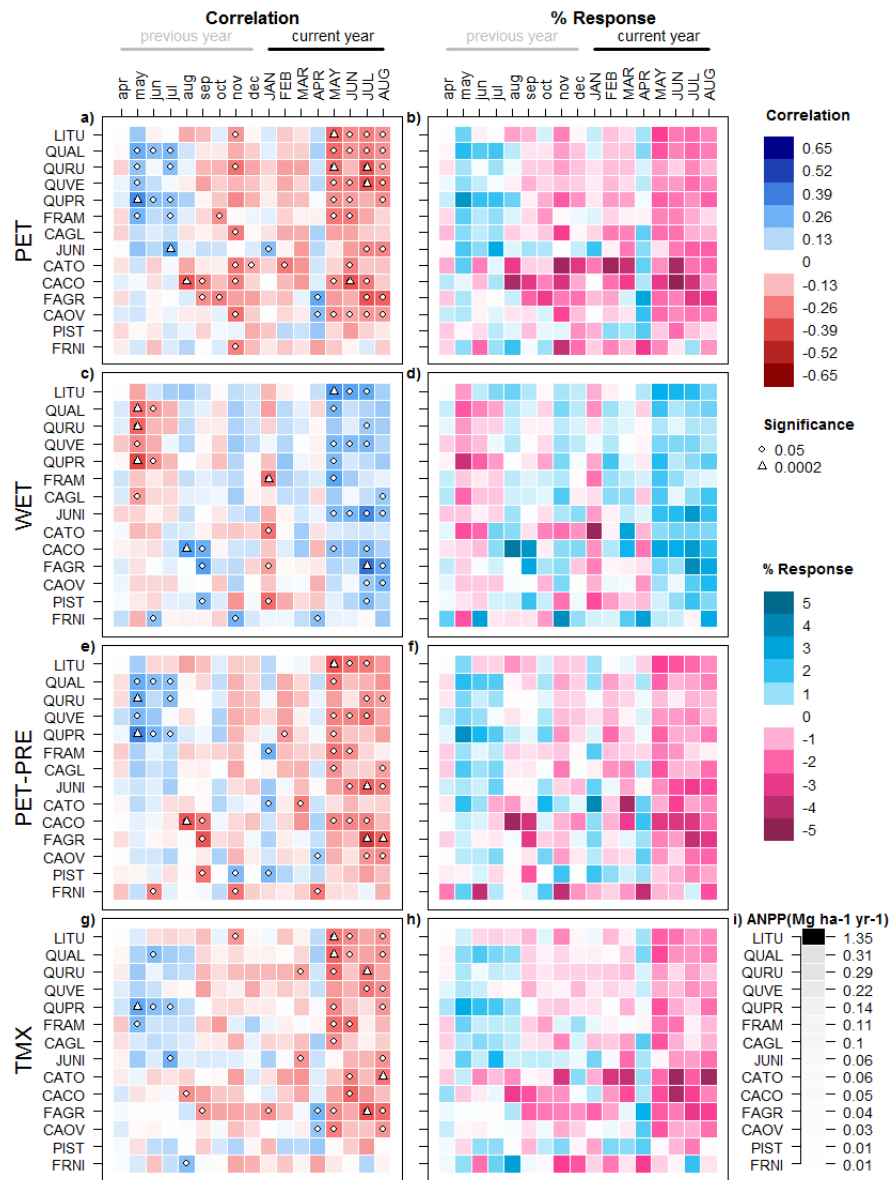
149x149mm (150 x 150 DPI)

Figure 2. Species' responses to four of the most influential climate variables analyzed here—potential evapotranspiration (a,b) wet day frequency (c,d), the difference between potential evapotranspiration and precipitation (e,f), and maximum temperature (g,h). Shown are Pearson correlations between ring width index and monthly climate variables (left panel) and percent response of growth and Aboveground woody Net Primary Productivity (ANPPstem) to +1 Standard Deviation (SD) in the climate variable (right panel). Also shown is ANPPstem of each species (i). Refer to Table 2 for species specific code information.
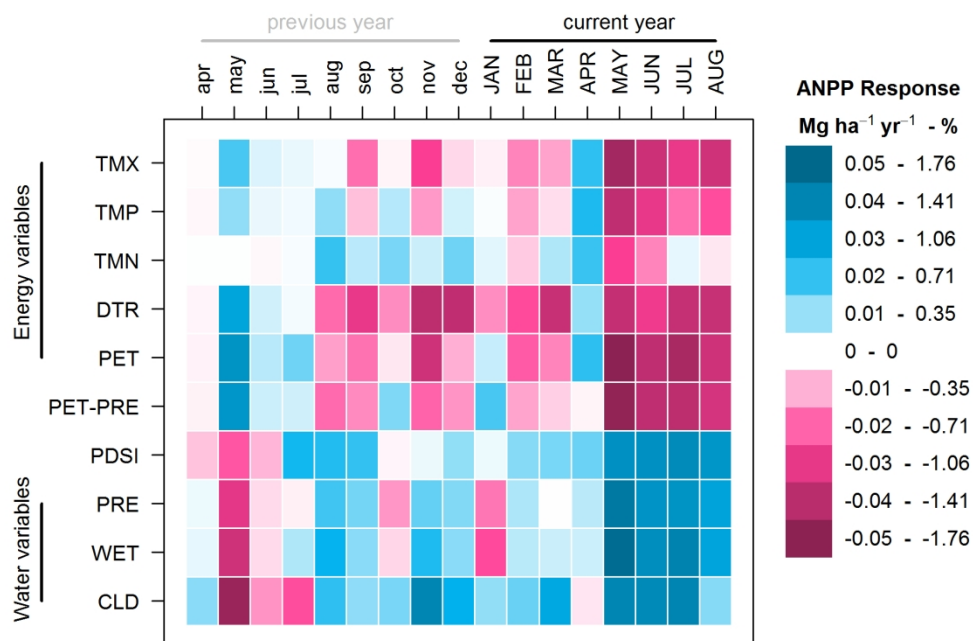
139x189mm (150 x 150 DPI)

Figure 3. Sensitivity of Aboveground woody Net Primary Productivity (ANPPstem) to 10 climate variables from 1901-2009. Shown is change in ANPPstem (Mg C ha-1 yr-1 and % of total) with +1 Standard Deviation (SD) in climate variable, as predicted based on the responses of individual species and the 2008 census of the Smithsonian Conservation Biology Institute (SCBI) ForestGEO plot.
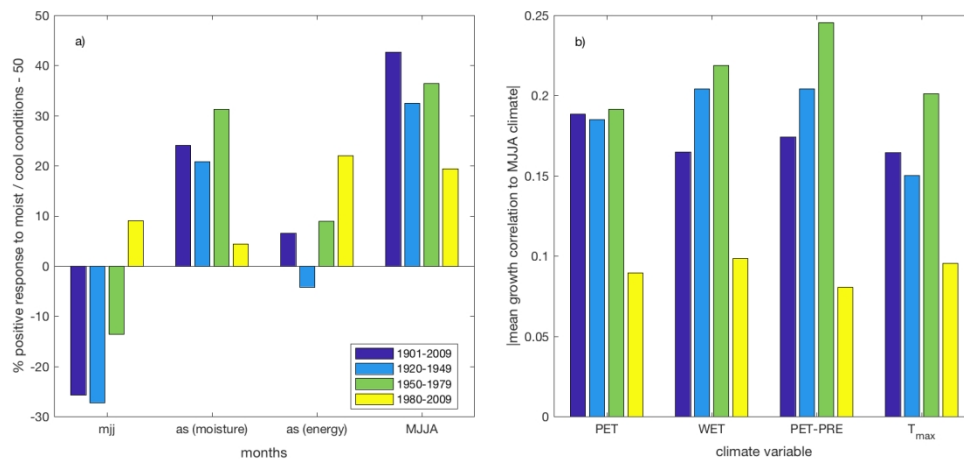
168x119mm (300 x 300 DPI)

Figure 4. Comparison of the (a) consistency and (b) average strength of climate correlations across the time periods analyzed here. Panel (a) shows the percent of species-climate variable-month combinations for which Pearson correlations are positive for moisture variables (PRE, WET, PDSI, CLD) and negative for energy variables (TMAX, TMP, TMIN, DTR, PET, PET-PRE) in each of 3 time periods: previous year's early growing season (mjj), previous year's late growing season (as), and current peak growing season (MJJA). Panel (b) shows the mean absolute correlation of growth to several climate variables of all species over MJJA. Refer to Table 1 for explanations of moisture and energy variables.
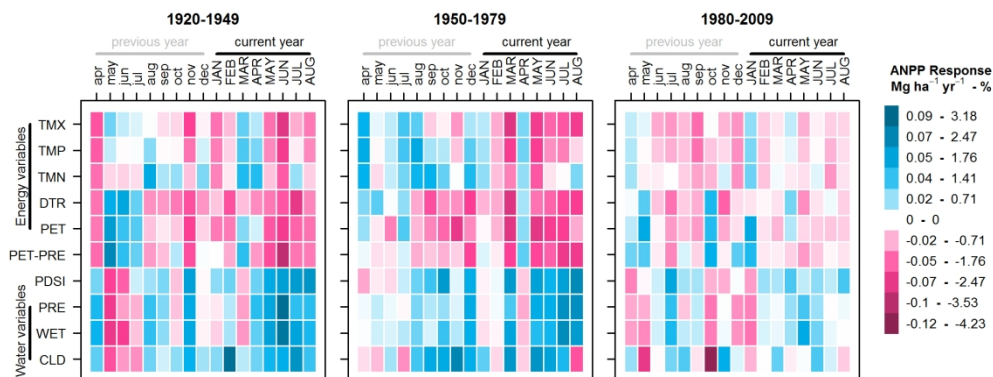
Figure 5. Predicted response of Aboveground woody Net Primary Productivity (ANPPstem) to +1 Standard Deviation (SD) change in 10 climate variables, as predicted based on the responses of individual species over three 30-year time periods and the 2008 census of the Smithsonian Conservation Biology Institute (SCBI) ForestGEO plot.

179x69mm (300 x 300 DPI)